

Ground State of the Spin-1/2 Kagome Lattice Heisenberg Antiferromagnet

Rajiv R. P. Singh

Department of Physics, University of California, Davis, CA 95616, USA

David A. Huse

Department of Physics, Princeton University, Princeton, NJ 08544, USA

(Dated: November 7, 2018)

Using series expansions around the dimer limit, we find that the ground state of the spin-1/2 Heisenberg Antiferromagnet on the Kagome Lattice appears to be a Valence Bond Crystal (VBC) with a 36 site unit cell, and ground state energy per site $E = -0.433 \pm 0.001J$. It consists of a honeycomb lattice of ‘perfect hexagons’. The energy difference between the ground state and other ordered states with the maximum number of ‘perfect hexagons’, such as a stripe-ordered state, is of order $0.001J$. The expansion is also done for the 36 site system with periodic boundary conditions; its energy per site is $0.005 \pm 0.001J$ lower than the infinite system, consistent with Exact Diagonalization results. Every unit cell of the VBC has two singlet states whose degeneracy is not lifted to 6th order in the expansion. We estimate this energy difference to be less than $0.001J$. The dimerization order parameter is found to be robust. Two leading orders of perturbation theory give lowest triplet excitations to be dispersionless and confined to the ‘perfect hexagons’.

PACS numbers: 75.10.Jm

The spin-1/2 antiferromagnetic Kagome-Lattice Heisenberg Model (KLHM) with Hamiltonian,

$$\mathcal{H} = J \sum_{\langle i,j \rangle} \mathbf{S}_i \cdot \mathbf{S}_j, \quad (1)$$

is a highly frustrated quantum spin model [1]. Its properties have been studied by a wide variety of numerical and analytical techniques [2, 3, 4, 5, 6, 7, 8, 9]. Yet, the precise nature of the ground state remains a subject of debate. Proposals have included a number of Valence Bond Crystals (VBC) [10, 11, 12, 13] as well as spin-liquid states with algebraic correlations [14, 15]. Recent experimental work on the material $\text{ZnCu}_3(\text{OH})_6\text{Cl}_2$ has attracted further interest to this model [16, 17, 18, 19], although this material is likely to also have significant Dzyaloshinski-Moria anisotropy. [20]

Here, we show that the ground state of KLHM appears to be a Valence Bond Crystal with a 36 site unit cell. It consists of a Honeycomb lattice of perfect hexagons as initially proposed by Marston and Zeng [10], discussed in more detail by Nikolic and Senthil [12], and shown in Fig 1. In a dimer covering, all triangles that have a singlet valence bond are locally in a ground state. As can be readily shown, any dimer covering leaves one-fourth of all triangles in the Kagome lattice empty. All quantum fluctuations in the ground state originate from these empty triangles, since it is only there that the singlet dimer covering is not locally a ground state of the Hamiltonian.

We develop series expansions around an arbitrary dimer covering of the infinite lattice using a Linked Cluster method [21] and compare the energies of various dimer coverings. To carry out the expansions, all (“strong”) bonds that make up the dimer covering are given an interaction strength J and all other (“weak”) bonds are given a strength λJ . Expansions are then carried out in powers of λ and extrapolated to $\lambda = 1$ where

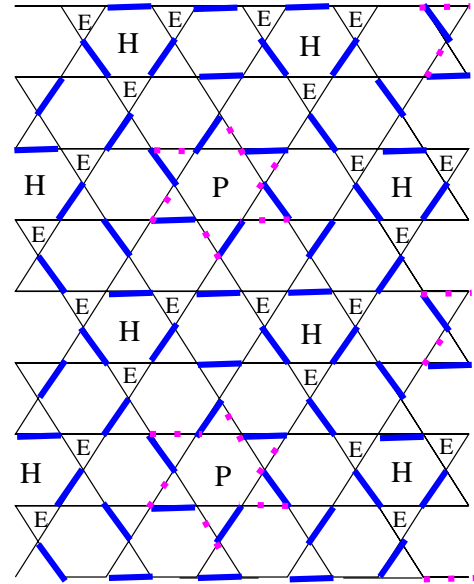


FIG. 1: (Color online) Ground state ordering pattern of low-energy (“strong”) bonds (blue) for the Kagome Lattice Heisenberg Model. The perfect hexagons are denoted as H, the empty triangles by E and the pinwheels as P. The two dimer coverings of the pinwheels that remain degenerate to high orders of perturbation theory are denoted by thick solid (blue) and dotted (magenta) bonds.

all bonds are equivalent in the Hamiltonian. Following recent development of the Numerical Linked Cluster scheme [22], we group together all weak bonds belonging to each triangle. This significantly simplifies the calculations: only 5 graphs contribute to the ground state energy to 5th order in λ (see Fig 2). The resulting series

expansion for the ground state energy shows surprisingly rapid convergence even at $\lambda = 1$.

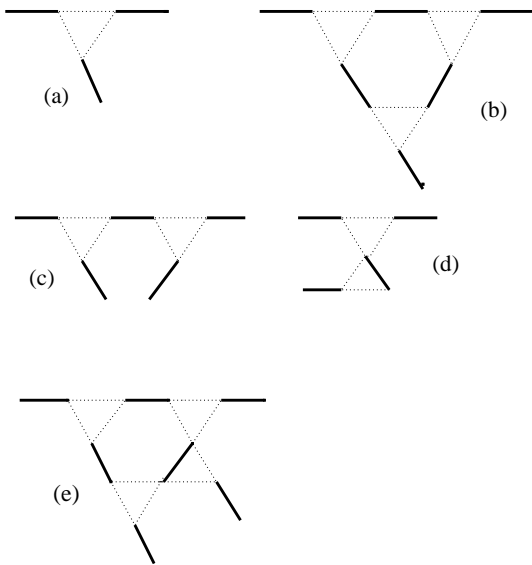


FIG. 2: Topologies of the graphs that contribute to the ground state energy to 5th order of perturbation theory. Graphs (a), (b), (c), (d), and (e) begin contributing in orders 2nd, 3rd, 4th, 4th, and 5th, respectively.

To 2nd order in our expansion for the ground state energy, all dimer coverings have the same energy. At 0th order, the singlet dimers each have energy $-0.75 J$. These dimers can lower their energy further by “resonating”, but only on the empty triangles. At 2nd order, these pairwise dimer-dimer interactions lower the energy by $0.28125 J$ per empty triangle. The degeneracy of all the dimer configurations is finally lifted at third order, where there is binding of 3 empty triangles into “perfect hexagons”; the 3 dimers around a perfect hexagon (see Fig. 2(b)) can then resonate together. This process lowers the energy of each perfect hexagon at 3rd order by $0.0703125 J$. At 4th order, resonances between two empty triangles when they are connected by a single dimer bond as in Fig. 2(c) produce an additional binding energy of amount $0.01953125 J$.

Thus at 4th order in our expansion we find that the ground state comes from the dimer covering with the maximum number of perfect hexagons, with neighboring hexagons arranged such that their empty triangles share a dimer bond as much as possible. It follows that once the positions and dimer coverings of two neighboring perfect hexagons are picked, the rest uniquely fall on a Honeycomb lattice of perfect hexagons. Furthermore, the dimerizations of all hexagons are simple translations of one another. This leads to the Valence Bond Crystal (VBC) arrangement shown in Fig. 1. For an infinite lattice, the ground state of this array of perfect hexagons is 24-fold degenerate, with 12 distinct translations, each of which has 2 reflections. As shown in Fig. 1, the arrange-

ment into this VBC also leaves a “pinwheel” of dimers in every unit cell. There are two degenerate pinwheel dimer coverings, and this degeneracy is not lifted to quite high orders of perturbation theory, implying that in a lattice of N sites there are at least $2^{N/36}$ states whose energy difference, per site, is much less than $0.001 J$.

We have carried the expansion to 5th order for the ground state energy. For the infinite lattice, the contribution at 5th order is quite small (about $0.0005 J$ per site) and slightly increases the energy difference between the honeycomb and stripe VBC [12] that was established at 4th order.

In addition to carrying out the expansions for the infinite system, one can also study the ground state properties of finite systems using the series expansion techniques. The 36 site cluster with periodic boundary conditions (PBC) studied by Leung and Elser [4] and Lecheminant *et al.* [6], does accommodate the unit cell of the Honeycomb VBC but not that of the stripe VBC. For the honeycomb VBC dimer covering on this cluster, the energy agrees with the infinite system through 3rd order. However, at 4th order there are additional graphs that enter due to the periodic boundary conditions, permitting 4 dimers to resonate along a path through 4 empty triangles that winds once around the periodic boundaries. From comparing the series through 5th order and using simple Pade estimates, we find the ground state energy for the 36 site cluster to be lower than that of the infinite system by $0.005 \pm 0.001 J$ per site, consistent with the Exact Diagonalization result of an energy of $-0.438377 J$ per site [4].

The $\lambda = 1$ energies for the infinite-lattice Honeycomb VBC, the stripe VBC of Nikolic and Senthil [12], and for the finite 36 site cluster with PBC and honeycomb VBC are listed in Table I, summed through 5th order. Note the apparently rapid convergence of the series, especially for the infinite lattice VBC states.

TABLE I: Ground state energy per site in units of J for various dimer states in perturbation theory. At each order we sum the contributions through that order for $\lambda = 1$.

Order	Honeycomb VBC	Stripe VBC	36-site PBC
0	-0.375	-0.375	-0.375
1	-0.375	-0.375	-0.375
2	-0.421875	-0.421875	-0.421875
3	-0.42578125	-0.42578125	-0.42578125
4	-0.431559245	-0.43101671	-0.43400065
5	-0.432088216	-0.43153212	-0.43624539

For the 36 site cluster, our considerations imply 48 spin-singlet states with very low energies per site within of order $0.001 J$ of the ground state, 24 corresponding to the ground state degeneracy of the thermodynamic system and 2 each for the pin-wheel states. But the other 48 states with two ‘perfect hexagons’ should also fall below the lowest triplet state, whose excitation energy for the

36 site cluster translates to a per site value larger than $0.004 J$. In the Exact Diagonalization studies about 180 singlet states are found below the lowest triplet. Since the binding energy for a perfect hexagon translates into a per site energy of $0.002 J$ for the 36 site cluster, some singlet states with only one perfect hexagon presumably can also have energies below the triplet gap in that cluster.

We have also studied the local bond energies to 3rd order in perturbation theory. To this order only four types of nearest neighbor bonds, representing only 27 of the 72 bonds per unit cell, have their expectation values changed from the 0th order values of $-0.75 J$ for strong bonds and 0 for weak bonds. These are: bond type A, the strong bonds inside the perfect hexagons; bond type B, the weak bonds inside the perfect hexagons; bond type C, the weak-bonds in the empty triangles which do not form part of the hexagon; and bond type D, the strong bonds that join two empty triangles between perfect hexagons. Their expectation values are listed in Table II. The total ground state energy is about $-0.22 J$ per bond. Although the series for the total energy is converging quickly to this value, the energies of individual bonds remain very different, as is expected for a valence bond crystal.

TABLE II: Expectation values $\langle S_i \cdot S_j \rangle$ for various bond types

Bond	0th order	2nd order	3rd order
A	-0.75	-0.5625	-0.515625
B	0	-0.1875	-0.257812
C	0	-0.1875	-0.1875
D	-0.75	-0.5625	-0.5625

Leung and Elser[4] had also calculated the energy-energy correlations in the ground state of the 36 site cluster. They had noted that the correlations at largest distances qualitatively matched the Valence Bond Crystal pattern after averaging over the 48 degenerate states. However, on a quantitative level there was no correspondence with the VBC, as the dimerization pattern seen in the Exact Diagonalization was considerably weaker. The modified values of the bond energy expectation values, calculated by us, do not significantly change this conclusion. We believe the reason for the discrepancy is the following: In the 36 site cluster, energy-energy correlations do not factorize even at the largest distances. Due to the Periodic Boundary Conditions, even bonds which are furthest away on the 36 site cluster can get correlated already in 2nd order of perturbation theory. Thus it is not appropriate to simply compare correlations $\langle (\vec{S}_i \cdot \vec{S}_j)(\vec{S}_k \cdot \vec{S}_l) \rangle$ to the products $\langle \vec{S}_i \cdot \vec{S}_j \rangle \langle \vec{S}_k \cdot \vec{S}_l \rangle$. In the future, we hope to calculate and compare the energy-energy correlations for the thermodynamic system and the 36 site cluster within this dimer expansion.

We have also calculated two leading orders of perturbation theory for the triplet excitation spectra. There are 18 elementary triplet excitations per unit cell, corre-

sponding to the 18 dimers. In 0th order, these triplets are dispersionless and have excitation energy J . To second order in perturbation theory, only 9 of the 18 triplets, consisting of the six belonging to the two perfect hexagons, and the three that couple the perfect hexagons via empty triangles, become dispersive and form a network on which excitations can move. The other 9 triplets, consisting of the 6 pinwheel dimers and the 3 other dimers that do not touch empty triangles, can only perform virtual hops at this order and thus remain dispersionless. The effective Hamiltonian for the nine dispersive states can be expressed in terms of a 9×9 matrix. Let $z_1 = \exp i\vec{k} \cdot \vec{r}_1$ with $\vec{r}_1 = -4\sqrt{3}\hat{y}$, and $z_2 = \exp i\vec{k} \cdot \vec{r}_2$ with $\vec{r}_2 = -6\hat{x} - 2\sqrt{3}\hat{y}$, and z_1^* and z_2^* be their complex conjugates, with the lattice oriented as in Fig. 1, with a nearest-neighbor spacing of unity. Then, in second order perturbation theory, the triplet excitation energies are the eigenvalues of the matrix

$$\Delta/J = (1 - \frac{5}{8}\lambda^2) + (\frac{1}{4}\lambda + \frac{1}{8}\lambda^2)M_1 + (\frac{1}{32}\lambda^2)M_2, \quad (2)$$

where the matrices M_1 and M_2 as a function of z_1 and z_2 are given in Table III and IV.

TABLE III: Matrix M_1

0	-1	-1	-1	1	0	0	0	0
-1	0	-1	1	0	-1	0	0	0
-1	-1	0	0	-1	1	0	0	0
-1	1	0	0	0	0	-1	0	1
1	0	-1	0	0	0	0	z_1	$-z_1$
0	-1	1	0	0	0	z_2	$-z_2$	0
0	0	0	-1	0	z_2^*	0	-1	-1
0	0	0	0	z_1^*	$-z_2^*$	-1	0	-1
0	0	0	1	$-z_1^*$	0	-1	-1	0

Note that this implies that two triplets have the lowest energy and they are each confined to one of the two perfect hexagons and thus remain dispersionless. The triplet gap becomes $1 - (1/2)\lambda - (7/8)\lambda^2$, which adds up to $-3/8$ at $\lambda = 1$ if we truncate at this order. This can be understood as arising from two factors: The hexagon is like a one-dimensional Alternating Heisenberg Chain and in that case the gap is known to be $1 - (1/2)\lambda - (3/8)\lambda^2$ [23]. There is a slight difference here with respect to the Alternating Heisenberg Chain because of the additional neighbors. The diagonal term is doubled but the second neighbor hop is absent, so that the overall result for the gap is the same. In addition, each strong bond has its two ends both connected to the same end of another dimer to which a triplet on that strong bond may make a virtual hop. This is like the triplets in the Shastry-Sutherland model [24, 25]. Due to this, and the fact that no such process happens in the ground state, there is a dispersionless reduction of the spin gap of magnitude $-(1/2)\lambda^2$. At 2nd order these two types of contributions simply add. Thus we find that although the series for

the ground state energy shows apparently strong convergence, the series for the spin gap does not, although the latter statement is about only the first two orders in the expansion. Further study of the triplet excitations is left for future work.

Our results have important implications for the finite temperature properties of the model. First of all, since the difference in energy of the Honeycomb VBC state and other dimer states (such as stripes) is less than $0.001J$ per site, any finite temperature transition in to a Honeycomb VBC phase should occur at a temperature of this order or lower. Secondly, given the large number (24) of degenerate ordering patterns, the phase transition seems likely to be first order. Third, since the attraction between the empty triangles is only of order $0.02J$, above $T \approx 0.02J$, all dimer configurations should have comparable Boltzmann weight, giving rise to a dimer liquid regime at intermediate temperatures. Fourth, the spe-

cific heat and entropy of the KLHM should have structure down to $T/J < 0.001$. It was found in the high temperature expansion study [5] that a naive extrapolation of the high temperature series down to $T = 0$ led to a finite ground state entropy. Furthermore, several studies have suggested multiple peaks in the specific heat [9, 26]. Our work shows at least $2^{N/36}$ very low energy states of the ‘pinwheels’, for an N -site system, and many other very low lying states, giving further support to these results.

Acknowledgments

This work was supported by the US National Science Foundation, Grants No. DMR-0240918 (R. S.) and DMR-0213706 (D. H.) and PHY05-51164.

TABLE IV: Matrix M_2

0	0	0	1	-1	0	-1	$-z_2$	$1+z_2$
0	0	0	-1	0	1	$1+z_1$	$-z_1$	-1
0	0	0	0	1	-1	$-z_1$	z_1+z_2	$-z_2$
1	-1	0	0	$1+z_2^*$	$1+z_1^*$	1	0	-1
-1	0	1	$1+z_2$	0	$1+z_1^*z_2$	0	$-z_2$	z_2
0	1	-1	$1+z_1$	$1+z_1z_2^*$	0	$-z_1$	z_1	0
-1	$1+z_1^*$	$-z_1^*$	1	0	$-z_1^*$	0	0	0
$-z_2^*$	$-z_1^*$	$z_1^*+z_2^*$	0	$-z_2^*$	z_1^*	0	0	0
$1+z_2^*$	-1	$-z_2^*$	-1	z_2^*	0	0	0	0

- [1] For a recent review see C. Lhuillier, arXiv:cond-mat/0502464.
- [2] C. Zeng and V. Elser, Phys. Rev. B **42**, 8436 (1990).
- [3] R. R. P. Singh and D. A. Huse, Phys. Rev. Lett. **68**, 1766 (1992).
- [4] P. W. Leung and V. Elser, Phys. Rev. B **47**, 5459 (1993).
- [5] N. Elstner and A. P. Young Phys. Rev. B **50**, 6871 (1994).
- [6] P. Lecheminant, B. Bernu, C. Lhuillier, L. Pierre and P. Sindzingre, Phys. Rev. B **56**, 2521 (1997).
- [7] F. Mila, Phys. Rev. Lett. **81**, 2356-2359 (1998).
- [8] C. Waldtmann, H. U. Everts, B. Bernu, C. Lhuillier, P. Sindzingre, P. Lecheminant and L. Pierre, Eur. Phys. J. B **2**, 501 (1998).
- [9] G. Misguich and B. Bernu, Phys. Rev. B **71**, 014417 (2005).
- [10] J. B. Marston and C. Zeng, J. Appl. Phys. **69**, 5962 (1991).
- [11] A. V. Syromyatnikov and S. V. Maleyev, Phys. Rev. B **66**, 132408 (2002).
- [12] P. Nikolic and T. Senthil, Phys. Rev. B **68**, 214415 (2003).
- [13] R. Budnik and A. Auerbach, Phys. Rev. Lett. **93**, 187205 (2004).
- [14] M. Hermele, T. Senthil, and M. P. A. Fisher, Phys. Rev. B **72**, 104404 (2005).
- [15] Y. Ran, M. Hermele, P. A. Lee, and X. -G. Wen, Phys. Rev. Lett. **98**, 117205 (2007).
- [16] J. S. Helton, K. Matan, M. P. Shores, E. A. Nytko, B. M. Bartlett, Y. Yoshida, Y. Takano, A. Suslov, Y. Qiu, J.-H. Chung, D. G. Nocera, and Y. S. Lee, Phys. Rev. Lett. **98**, 107204 (2007).
- [17] O. Ofer, A. Keren, E. A. Nytko, M. P. Shores, B. M. Bartlett, D. G. Nocera, C. Baines, and A. Amato, cond-mat/0610540.
- [18] P. Mendels, F. Bert, M. A. de Vries, A. Olariu, A. Harrison, F. Duc, J. C. Trombe, J. Lord, A. Amato, and C. Baines, Phys. Rev. Lett. **98**, 077204 (2007).
- [19] T. Imai, E. A. Nytko, B. M. Bartlett, M. P. Shores, D. G. Nocera, cond-mat/0703141.
- [20] M. Rigol and R. R. P. Singh, Phys. Rev. Lett. **98**, 207204

- (2007).
- [21] J. Oitmaa, C. Hamer and W-H. Zheng, *Series Expansion Methods for strongly interacting lattice models*, (Cambridge University Press 2006).
- [22] M. Rigol, T. Bryant, and R. R. P. Singh, Phys. Rev. Lett. **97**, 187202 (2006).
- [23] A. B. Harris, Phys. Rev. B**7**, 3166 (1973).
- [24] B. S. Shastry and B. Sutherland, Physica B **108**, 1069 (1981).
- [25] W. H. Zheng, J. Oitmaa and C. J. Hamer, Phys. Rev. B**65**, 014408 (2002).
- [26] V. Elser, Phys. Rev. Lett. **62**, 2405 (1989).